Received: 11 July 2019 | Revised: 26 December 2019 | Accepted: 10 January 2020
DOI: 10.1002/aic.16913

REACTION ENGINEERING, KINETICS AND CATALYSIS

AIChE JOURNAL

Refinement of the kinetic model for guaiacol hydrodeoxygenation over platinum catalysts

Yang Xiao | **Rexonni Lagare** | **Lindsey Blanshan** | **Enrico N. Martinez** | **Arvind Varma**†

Davidson School of Chemical Engineering, Purdue University, West Lafayette, Indiana

Correspondence
Yang Xiao, Davidson School of Chemical Engineering, Purdue University, West Lafayette, IN 47907-2100.
Email: xiao63@purdue.edu

Funding information
the R. Games Slayter fund; the William and Cynthia Smith gift

Abstract

In our prior work (*Ind Eng Chem Res*, 2015, *54*, 10638-10644), hydrodeoxygenation (HDO) kinetics of guaiacol, a well-known model compound of bio-oil, over Pt/AC (activated carbon) catalysts were investigated under *integral* operating conditions. It was found that the pseudo-homogeneous plug-flow model utilizing these kinetics describes the experimental observations well (with normalized RMS error = 7.6%). In the present work, under *differential* operating conditions instead, we refine the kinetic model for the same reaction network over the same catalyst. We show that among the five reaction steps in the network, the reaction order of one step differs from our prior work, while the orders remain unchanged for the other four steps. The activation energies of two steps differ from our prior values by 10–15 kJ/mol, and for the other three steps remain essentially consistent with our prior work. The kinetic parameters from the present work are used to predict fixed-bed reactor performance under *integral* operating conditions as well. The comparison between experimental and predicted values for both the prior and new sets of data is excellent and even better than our prior model (with reduced normalized RMS error = 4.2%). The kinetic analysis additionally proposed that the direct and indirect pathways of phenol formation from guaiacol HDO depend on guaiacol conversion values. The present work demonstrates that kinetic expressions and parameters obtained from a gradientless differential reactor are more reliable and can be used to successfully predict integral reactor performance data.

KEYWORDS
differential reactor, guaiacol, hydrodeoxygenation (HDO), kinetics, Pt catalyst

1 | INTRODUCTION

The consumption of fossil fuels has increased significantly in the recent past, and the trend is likely to continue in the foreseeable future. Owing to increasing scarcity of crude oil on Earth and its related environmental issues, the need to develop renewable energy sources, for example, biomass, solar, wind, and hydrogen, has been strong.[1] Fast pyrolysis is a promising technology to obtain biofuels from various lignocellulosic materials, which are considered as the second generation biomass resources that do not compete with food supply for humans. The produced bio-oil, typically containing relatively high oxygen content, however, cannot be directly used as transportation fuels owing to poor stability, low heating value, and inferior combustion performance. To overcome these problems to satisfy specifications of transportation fuels, catalytic hydrodeoxygenation (HDO) has been widely investigated as an important approach to

---

†Deceased author.

upgrade pyrolysis-derived bio-oils, in which supported metal catalysts and hydrogen molecules are usually employed.[2-5]

The kinetics of bio-oil HDO play an important role in terms of investigating reaction pathways/mechanisms, reactor design, and process scale-up. Kinetic studies of catalytic HDO have been reported using various model compounds of bio-oil, such as m-cresol,[6-8] phenol,[9-11] anisole.[12] As used in our prior work[13] and literature,[14] guaiacol is a well-known model compound of lignin-derived bio-oil, owing its two representative types of oxygen-containing groups (—OH and —OCH_3). Two kinetic models, that is, the power-law and Langmuir–Hinshelwood–Hougen–Watson (LHHW), were developed for guaiacol HDO. Bhanawase et al developed a LHHW model for guaiacol HDO over a hydrotalcite catalyst,[15] and Leiva et al reported a similar LHHW model when the HDO reaction occurred over Re-based catalysts.[16] In addition, Nie and Resasco presented LHHW kinetics for the conversion of a similar model compound (m-cresol) over the Pt/SiO_2 catalyst.[6] On the other hand, the simple power-law model has been more frequently employed for kinetic modeling of guaiacol HDO. Interestingly, different reaction orders were reported for guaiacol conversion, including first-order for Pt/γ-Al_2O_3,[17,18] Ni-Cu,[19] Ni_2P,[20] second order for Pt/AC (activated carbon),[13] and even zero order for a Fe-based catalyst.[21]

To measure catalytic kinetics in the laboratory, continuous flow fixed-bed reactors are frequently used. These can be operated in either the differential or the integral mode. In a differential reactor, reactant conversions are typically kept under ~5–10%, thus reaction rates can be obtained directly by analyzing concentrations at inlet and outlet of the reactor, relative to the packed weight of catalyst.[22,23] For an integral reactor, however, reaction rates have to be obtained by differentiation of the conversion—contact time curve, thus leading to potential errors. In general, the kinetic measurement method needs to be free of temperature and concentration gradients (i.e., gradientless), ensuring that all measurements are performed at fixed fluid phase temperature and concentration of the reactants, facilitated by the differential mode of operation. On the other hand, since the difference between the feed and outlet concentrations is small for the differential mode, measurement errors can arise. Excellent reviews of laboratory reactors for kinetic measurements have been published in the literature.[24-26] Note that for the above investigations on kinetic modeling of guaiacol HDO, only two studies used a differential reactor,[17,18] while others employed the integral mode.[13,15,16,19-21]

Using guaiacol as a model compound of bio-oil,[27,28] our prior study presents that Pt/AC is an efficient catalyst for guaiacol HDO reaction, providing superior deoxygenation activity at relatively low operating temperature (less than 300°C) and atmospheric pressure.[29] Following this, under *integral* operating conditions, the reaction kinetics study was carried out, and kinetic parameters such as rate constants and activation energies were obtained for the various reaction steps (see Figure 1).[13] It was found that the developed model describes reaction kinetics well, with a root-mean-square (RMS) error of 7.6% versus experimental data. In this work, we refine the kinetic model by conducting the reaction kinetic studies under *differential* operating conditions (i.e., using a differential reactor). This refined model showed an even better fit as compared to the experimental data and our prior model, reducing the RMS from 7.6 to 4.2%. Interestingly, some reaction order and activation energy values are different as compared with those obtained with our prior integral method. Possible reasons for these differences are discussed in this article.

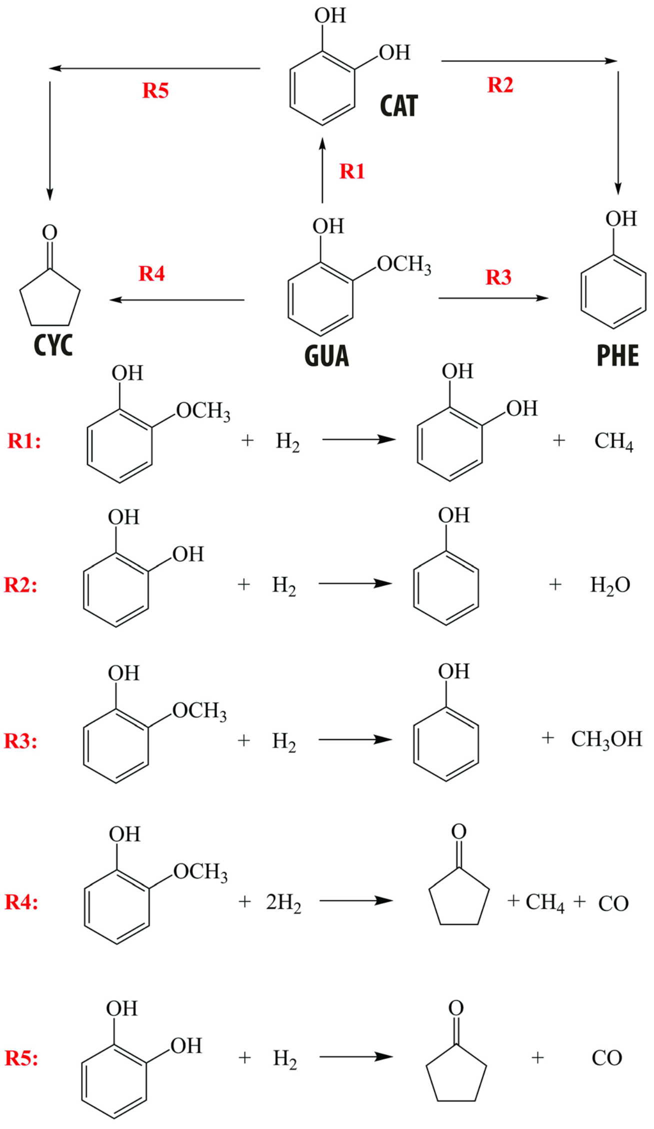

FIGURE 1 Proposed reaction network and pathway of guaiacol hydrodeoxygenation over Pt/AC catalysts [Color figure can be viewed at wileyonlinelibrary.com]

2 | METHODS

2.1 | Experimental

The chloroplatinic acid hexahydrate (99.9% metal basis) from Sigma Aldrich was used as the Pt precursor. The 80–120 mesh AC support was from Norit Americas Inc. The Pt catalysts were prepared by the wet impregnation method as described in our prior works.[30,31] Guaiacol (GUA), catechol (CAT), phenol (PHE), and cyclopentanone (CYC) with purity all >98.0% were obtained from Alfa Aesar. Ultrahigh purity grade gases (O_2, Ar, N_2, He, and H_2, all >99.9%) were purchased from Indiana Oxygen. The catalytic performance tests were conducted in a continuous flow fixed-bed reactor setup, as used in our prior studies.[13,29] Prior to tests, the catalyst was activated and reduced at 350°C and 1 atm for 3 hr under a gas mixture flow (H_2: N_2 = 1:2) of 100 ml/min. The reactor was then purged using 50 ml/min N_2 for 20 min. The following standard operating conditions were used: 275°C, 1 atm total pressure, 20–50 mg catalyst for differential reactions (conversions typically <10%) and 500 mg catalyst for integral reactions (conversions >10%), total gas (H_2: N_2 = 1:1) flow rate 100 ml/min, and guaiacol feed rate 0.025 ml/min (liquid, at room temperature). For differential reactions, to reach relatively long catalyst bed for plug-flow, unsupported inert AC was used to dilute the catalyst. The feed flow rates correspond to a molar ratio of 10:1 H_2: guaiacol. Differential/integral conditions were achieved by the varying packed amount of catalyst. Blank tests of the AC support without Pt loading were conducted under the standard reaction conditions, and guaiacol conversion was less than 0.2%. All experiments had carbon mass balances, including both liquid and gas phases, of 92 ± 2% for both liquid and gas phases. Similar to the literature.[32,33] Unless stated otherwise, all data sets were taken at 10 min time on stream (TOS) as initial reaction rates. Note that these catalysts are also stable at longer TOS (e.g., 5 hr).[29] Similar to our prior work,[13,31,34] an Agilent GC6890 equipped with an FID and a DB-1701 column (30 m × 0.25 mm) was used for quantitative analysis of the liquid products. The gaseous effluent was analyzed using an Agilent 3000 A Micro-GC equipped with two columns (Column A: MolSieve 5 A, 10 m × 0.32 mm; Column B: Plot U, 8 m × 0.32 mm) and a thermal conductivity detector.

2.2 | Kinetic model development

As presented by Equation (1), the power-law model was used to describe the relation between reaction rates and partial pressures of reactants (guaiacol and catechol for different reaction steps in Figure 1).

$$r_i = k_i\, p_i^{n_i} \tag{1}$$

where p_i is the partial pressure of guaiacol (p_{GUA}) for Steps R1, R3, and R4; p_i is the partial pressure of catechol (p_{CAT}) for Steps R2 and R5.

Taking logarithm of both sides yields Equation (2) as follows.

$$\log(r_i) = n_i \log(p_i) + \log(k_i) \tag{2}$$

In later sections, $\log(r_i)$ and $\log(p_i)$ are plotted to fit reaction orders (n_i).

3 | RESULTS AND DISCUSSION

Before kinetic measurements were carried out, the plug-flow condition was confirmed since the well-known criterion (the reactor diameter must be at least 10 times the catalyst particle diameter, and the catalyst bed length should be at least 50 times the particle diameter) was satisfied.[35] Specifically, the reactor inner diameter is more than 15 times the catalyst particle size, and the height of catalyst packing bed is more than 60 times the catalyst particle size. The absence of mass-transfer limitations, including both internal and external diffusion, was also confirmed by satisfying the Weisz and Prater criterion[2,36] as follows: $\left(\frac{d_p^2 r_i \rho_{cat}}{C_i D_{\mathrm{eff}}} < 1\right)$. The Mears criterion was used to exclude heat-transfer effects $\left(\frac{r_i \Delta H_i \rho_{\mathrm{cat}} d_p E_{a_i}}{hRT^2} < 0.15\right)$.[37]

Note that only one catalyst, 5% Pt/AC, was used in this study, which has been previously well characterized by various techniques, including TEM, TGA,[29] chemisorption, BET, AES-ICP, H_2-TPD, and TPSR,[31] thus catalyst characterization results are not reported here.

3.1 | Effect of H_2 to guaiacol feed ratio

Under standard operating conditions, in the present work as well as in our prior work,[29] the molar ratio of hydrogen to guaiacol feed was 10:1. Owing to excess hydrogen, the contribution of hydrogen to reaction rate was considered to be zero order.[13] To investigate the hydrogen feed effect, in the present section, the molar ratio of hydrogen and guaiacol was varied in range 0–18. As shown in Figure 2, when hydrogen: guaiacol molar feed ratios were 0–2, negligible guaiacol conversion occurred, while when this ratio was 2–6, guaiacol exhibited ~3–50% conversion, producing catechol (non-deoxygenated species) and phenol (partially deoxygenated species) as the primary products. When the ratio was in the range 8–18, guaiacol reached essentially the same conversion (~90%), producing all three components (catechol, phenol, and cyclopentanone). These observations indicate that excess hydrogen (e.g., hydrogen: guaiacol molar ratio 8–18) is required to reach high HDO performance, and the assumption of to be zero order for hydrogen in the reaction rate is reasonable when the ratio is greater than 8.

3.2 | Reaction orders

The proposed reaction pathways, including five individual steps (R1–R5) as shown in Figure 1, were established under *integral* operating conditions.[29] When using guaiacol as feed, under *differential* operating conditions (guaiacol conversion less than 10%), all three products—catechol along with phenol and cyclopentanone were observed, that is, Steps R1, R3, and R4 prevailed. Instead, when catechol was used as feed, also under differential conditions, only phenol and cyclopentanone (corresponding to steps R2 and R5, respectively) existed in the liquid products. Interestingly, the same liquid phase products were found also when the reductant was methane instead of hydrogen.[31,34,38] These experimental observations imply that by feeding guaiacol and catechol separately, both under *differential* operating conditions, we can investigate two sets of reactions steps individually, including Set 1 (Steps R1 along with R3 and R4) and Set 2 (Steps R2 along with R5). Also note that for each step of either set, the reaction

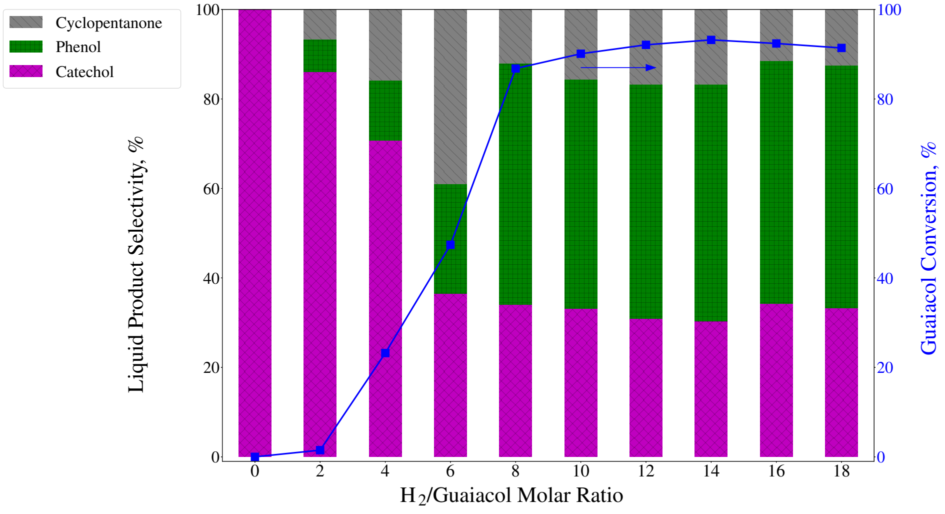

FIGURE 2 Effect of hydrogen to guaiacol feed ratio over the 5% Pt/AC; 275°C, 1 atm, 0.5 g catalyst, total gas flow 100 ml/min with H_2:N_2 = 1:1, guaiacol liquid feed rate 0.025 ml/min, TOS = 10 min. TOS, time on stream [Color figure can be viewed at wileyonlinelibrary.com]

rate depends only on feed concentration (i.e., guaiacol for Set 1 and catechol for Set 2) and is independent of other species concentrations. Considering Set 1, the reactions rates of Steps R1, R3, and R4 in the network of Figure 1, depend only on guaiacol partial pressure. Similarly, the reactions rates of Steps R2 and R5 of Set 2 depend only on catechol partial pressure. Because differential operating conditions apply, the reaction rate values are obtained by Equation (3).

$$r_i = F_0 \times \frac{X_i}{W} \qquad (3)$$

Using the above Equations (2) and (3), plots of log(r_i) and log(p_i) at 275–350°C are shown in Figure 3. The slopes of these lines, corresponding to estimated reaction orders of Steps R1–R5 (n_1-n_5), are listed in Table 1. It appears that the estimated reaction orders of step R1 vary from 0.974–1.024, and the values for Steps R2–R5 are 0.943–1.005, 1.971–2.075, 1.897–2.020, and 0.968–1.035, respectively. Since all estimated reaction orders are close either to 1 or 2, as shown in Table 2, integer reaction orders were used for all five steps, that is, n_1 = 1, n_2 = 1, n_3 = 2, n_4 = 2, and n_5 = 1. Using these integer reaction orders, reaction rates and average (of feed and exit) reactant partial feed pressures are plotted in Figure 4, which demonstrates that integer reaction orders represent Experimental observations well at 275–325°C. In later sections, only integer reaction orders are used to model the kinetic behavior of catalytic guaiacol HDO.

Step R1 is a first-order reaction, which is consistent with the literature,[17-20] while our prior work[13] fitted a second order for the same step. This is likely because kinetic measurements were under integral (our prior work[13]) and differential (the present work) operating conditions, respectively. In fact, reaction order may vary over different catalysts and/or operating conditions. For Pt-based catalysts, both the nonacidic AC (activated carbon) support in the present work and acidic γ-Al_2O_3 support in the literature[17,18] give first order of guaiacol conversion. The Ni-based catalysts, including Ni-Cu[19] and Ni_2P,[20] show the same reaction order as well. Interestingly, the zero-order reaction was proposed over a Fe-based catalyst.[21] In addition to the power-law model, Leiva et al and Bhanawase et al developed LHHW models for the kinetics of guaiacol HDO. The present work suggests that a simple power-law model can predict guaiacol HDO kinetics adequately. Steps R3 and R4 appear to be second-order reactions, which are likely owing to the requirement of two reactant molecules for these steps while Steps R2 and R5 are both first orders, as consistent with our prior study.[13]

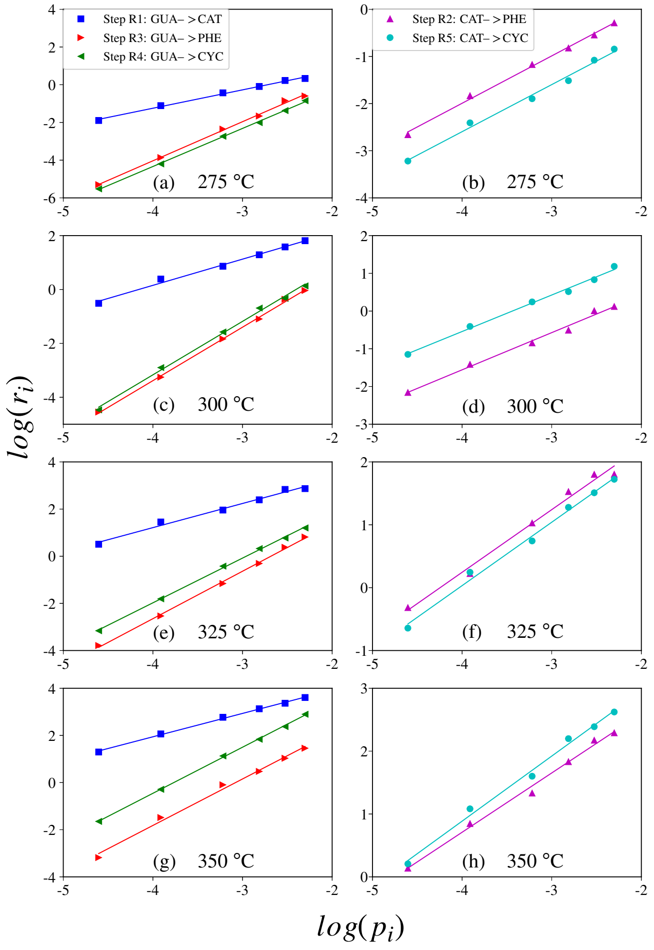

FIGURE 3 Fits of log(r_i) versus log(p_i) for Steps R1–R5 at 275–350°C—(a), (c), (e), (g) feed guaiacol, and (b), (d), (f), (h) feed catechol [Color figure can be viewed at wileyonlinelibrary.com]

3.3 | Activation energies

Using the well-known Arrhenius Equation (4), reaction activation energies (E_{a_i}) were calculated (Figure 5).

$$k_i = A_i \cdot \exp\left(-\frac{E_{a_i}}{R \cdot T}\right) \tag{4}$$

The E_{a_i} values, as well as integer reaction orders, are listed in Table 2 and also compared with our prior work,[13] where integral operating conditions were employed. In general, refinement of activation energies under *differential* operating conditions are consistent with our prior data obtained under integral operating conditions.[13] The largest differences of E_{a_i} values are 10 and 15 kJ/mol for Steps R2 and R4, respectively (about 10% difference). The activation energy of Step R1 was reported in the range of 58.7–89.1 kJ/mol for Co, Mo, and Cu catalysts.[19,39] As discussed in our prior study,[13] there are no experimental E_{a_i} data for guaiacol over Pt-based catalysts, while theoretical calculations estimated the E_{a_i} value of Step R1 to be 100 kJ/mol.[40]

3.4 | Predictions under integral conditions and parity plot

From former sections, all kinetic parameters, including reaction orders, rate constants, and activation energies, are known for all steps (R1–R5) under differential operating conditions. It is worth using these to predict reactor performance under integral operating conditions (plug-flow), and comparing with the corresponding experimental results. A comparison of the experimental (differential and integral, filled symbols) and predicted reactor outlet flow rates for all four species (guaiacol, catechol, phenol, and cyclopentanone) is shown in Figure 6, where guaiacol conversions range from 2 to 92%. It summarizes the goodness-of-fit in a parity plot. The values for all four species are close to the diagonal line and relatively evenly distributed on both sides, indicating a good fit (normalized RMS error = 3.7%). For comparison, the experimental data from our prior work[13] obtained under integral conditions (open symbols, guaiacol conversions 52–96%) is also shown in Figure 6, where the predicted values utilize the kinetic parameters obtained in the current work. These data also show a better fit (normalized RMS error = 4.2%) as compared to our prior model developed under *integral* operating conditions (normalized RMS error = 7.6%), thus indicating the reliability of the kinetic parameters.

TABLE 1 Reaction orders obtained from fitting log(r_i) versus log(p_i)

Fitted reaction orders	275°C	300°C	325°C	350°C
n_1	0.974	0.972	1.024	0.992
n_2	1.005	0.986	0.996	0.943
n_3	2.075	1.984	2.012	1.971
n_4	2.020	1.984	1.897	1.955
n_5	0.998	0.968	1.008	1.035

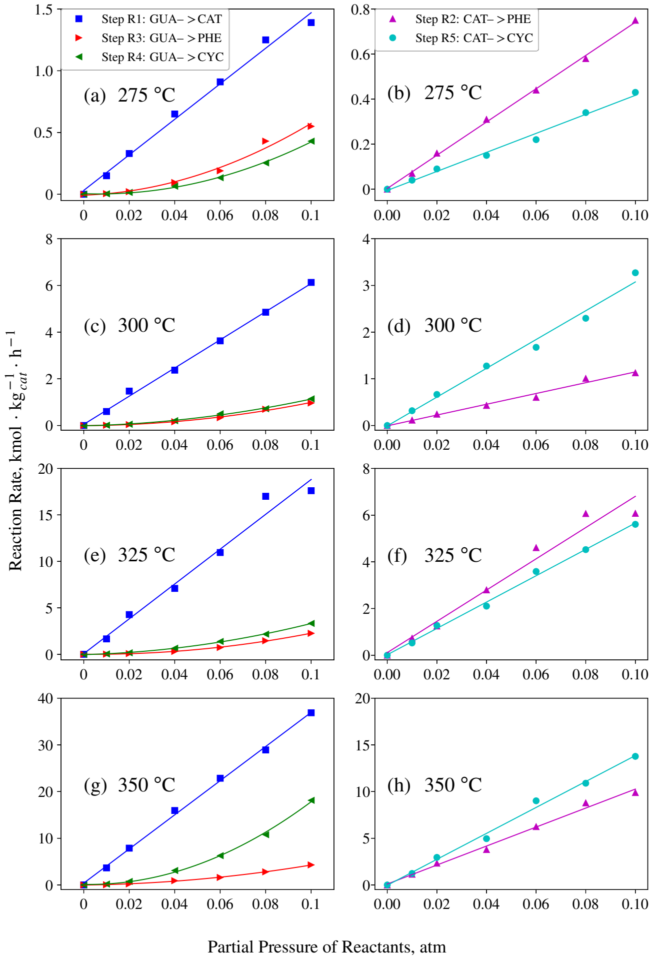

FIGURE 4 Reaction rate fits using integer reaction orders, that is, $n_1 = n_2 = n_5 = 1.0$, $n_3 = n_4 = 2.0$, for Steps R1–R5 at 275–350°C—(a), (c), (e), (g) guaiacol feed; (b), (d), (f), (h) catechol feed [Color figure can be viewed at wileyonlinelibrary.com]

TABLE 2 Comparison of reaction orders and activation energies between integral and differential approaches

	n_i		E_{a_i}, kJ/mol	
Reaction step	Present work	Prior work[13]	Present work	Prior work[13]
R1	1	2	124.1	125.5
R2	1	1	110.4	99.8
R3	2	2	84.8	92.7
R4	2	2	135.3	149.0
R5	1	1	129.1	124.6

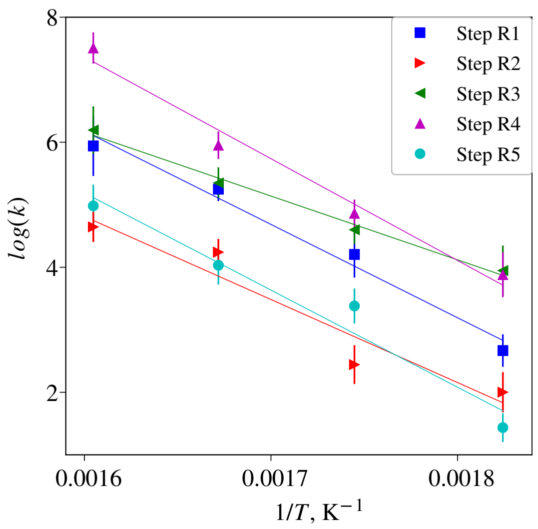

FIGURE 5 Arrhenius plots for the rate constants [Color figure can be viewed at wileyonlinelibrary.com]

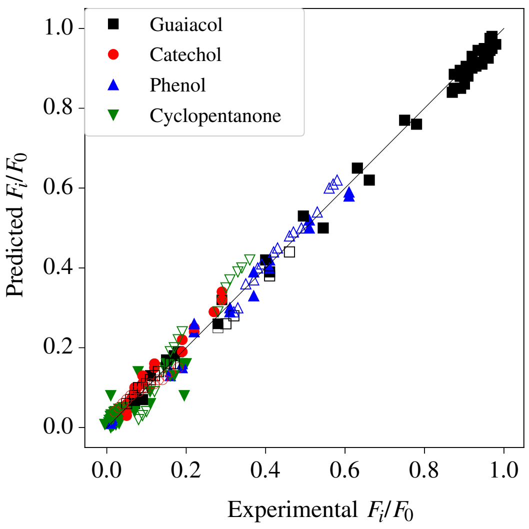

FIGURE 6 The parity plot of all investigated data; filled symbols—data of present work, open symbols—data of Reference 13 [Color figure can be viewed at wileyonlinelibrary.com]

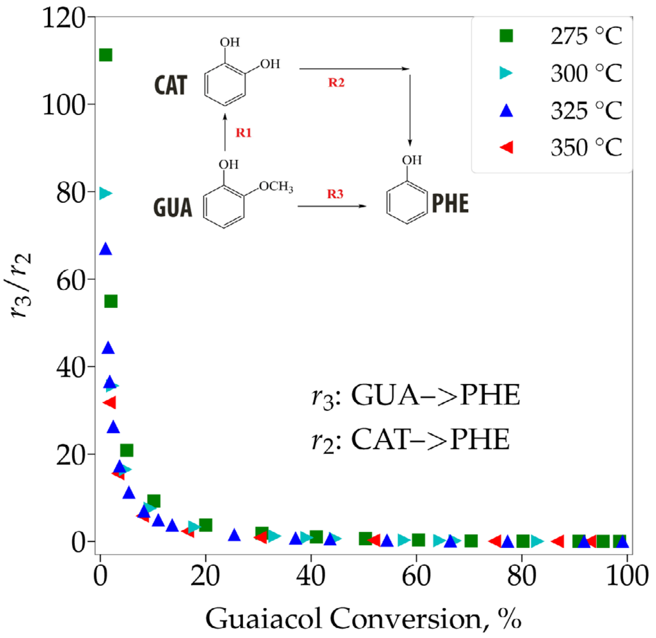

FIGURE 7 Reaction rate ratio of direct and indirect phenol formation pathways as a function of guaiacol conversion at 275–350°C; r_3 for direct pathway, r_2 for indirect pathway [Color figure can be viewed at wileyonlinelibrary.com]

3.5 | Pathway analysis of phenol formation

Phenol is widely reported as a primary product of guaiacol HDO, while the formation pathway of phenol is still under debate. As shown in Figure 1, two pathways exist for phenol formation.[41,42] The direct pathway refers to converting guaiacol to phenol without producing any intermediate (via Step R3, i.e., demethoxylation), and the indirect pathway typically generates catechol as an intermediate (via Steps R1 and R2, demethylation, i.e., DME). In fact, the actual pathway may vary over different catalysts (active site, supports) and operating conditions (e.g., temperature, H_2 pressure).[41] Based on experimental observations and kinetic analysis, the Gates group proposed the direct pathway for phenol formation over Pt catalysts supported on acidic γ-Al_2O_3.[17,18] As similar reaction mechanism was reported for Fe[21] and CoMoS/ZrO_2[43] catalysts. On the other hand, the Vlachos group proposed the indirect pathway on Pt(111) via DFT calculations.[44] One more mechanism on the basis of the indirect pathway was also found over Re,[16] Ru,[42] Ni,[20] and Au[45] catalysts. Interestingly, acidity of catalyst supports tune the pathway of phenol formation. It appears that acidic Al_2O_3, ZrO_2 supports promote the indirect pathways,[20,43] while nonacidic catalysts lead to the direct pathway.[41,46]

It is worth applying a kinetic analysis to investigate the phenol formation pathway. Since both Steps R3 and R2 in Figure 1 contribute to the reaction rate of phenol formation ($r_{PHE} = r_3 + r_2$), the ratio of these two reaction rates (i.e., r_3/r_2) is a descriptor of the individual contributions. Using the developed kinetic model in the present work, the plot of r_3/r_2 versus guaiacol conversion at 275–350°C is shown in Figure 7. It appears that at all investigated temperatures, r_3/r_2 decreases with guaiacol conversion increase. At low guaiacol conversion, r_3 is greater than r_2, owing to the relatively high guaiacol concentration, which indicates that the direct pathway functions as the primary route for phenol formation. At high guaiacol conversion, however, r_2 is faster than r_3, since catechol has accumulated to a significant concentration, leading the indirect pathway via catechol as the main way. In general, our kinetic analysis demonstrates that the pathway of phenol formation over the same catalyst and under the same operating conditions may vary at different guaiacol conversion values.

4 | CONCLUDING REMARKS

In our prior work, the kinetics of guaiacol HDO over Pt/AC catalysts were investigated under *integral* operating conditions. It was shown that the pseudo-homogeneous plug-flow model utilizing these kinetics describes the experimental observations well (normalized RMS error = 7.6%).[13] In the present work, we refine the kinetic model for the same reaction network over the same catalyst utilizing *differential* operating conditions. It is found that among the five reaction steps, the reaction order of one step (R1 in Figure 1) differs from our prior work, while reaction orders for the other four reactions remain unchanged. The activation energies of two steps (R2 and R4) differ from our prior data by 10–15 kJ/mol (about 10% difference), while the values for the other three steps remain essentially consistent. The kinetic parameters from the present work are used to predict fixed-bed reactor performance under integral operating conditions, from both our prior and current work. The comparison between the experimental and predicted values for both sets of data is excellent and even better than our prior model (with reduced normalized RMS error = 4.2%). The kinetic analysis additionally proposed that at low guaiacol conversion, the direct pathway (guaiacol to phenol without producing intermediate) prevails for phenol formation, while the indirect pathway (guaiacol to phenol via catechol as intermediate) is favored at high guaiacol conversion. This work demonstrates that for relatively simple reaction networks, it is possible to create sub-networks, for which kinetic expressions from gradientless conditions (e.g., differential operation) can be obtained in a straightforward manner. The kinetic parameters obtained under such conditions are more reliable and may be used to successfully predict integral reactor data.

ACKNOWLEDGMENTS

This work was supported by the R. Games Slayter fund and the William and Cynthia Smith gift funds.

NOTATION

A_i, (kmol/[$\text{kg}_{\text{cat}} \cdot \text{hr} \cdot \text{atm}^{n_i}$])	Pre-exponential factor of Step i when the reaction order is n_i
C_i, (kmol/m^3)	concentration of species i
D_{eff}, (m^2/hr)	effective diffusion coefficient
d_p, (m)	catalyst particle diameter
E_{a_i}, (kJ/mol)	activation energy of Step i
F_0, (kmol/hr)	total feed flow rate
h, (kJ/[m$^2 \cdot$ K $\cdot$ hr])	heat-transfer coefficient
k_i, (kmol/[$\text{kg}_{\text{cat}} \cdot \text{hr} \cdot \text{atm}^{n_i}$])	reaction rate constant of Step i when the reaction order is n_i
n_i, (–)	reaction order of Step i
p_i, (atm)	partial pressure of species i
R, (kJ/[K $\cdot$ kmol])	gas constant
r_i, (kmol/[$\text{kg}_{\text{cat}} \cdot \text{hr}$])	reaction rate of Step i
T, (K)	reaction temperature
W, (kg)	catalyst packing amount
X_i, (–)	conversion of Step i
ΔH_i, (kJ/mol)	enthalpy change of Step i
ρ_{cat}, (kg/m^3)	density of packed catalyst

ORCID

Yang Xiao https://orcid.org/0000-0003-1705-2213
Arvind Varma https://orcid.org/0000-0002-3472-5929

REFERENCES

1. Davis SJ, Lewis NS, Shaner M, Aggarwal S, Arent D, Azevedo I. Net-zero emissions energy systems. *Science*. 2018;360(6396):eaas9793. https://doi.org/10.1126/science.aas9793.
2. Wan H, Chaudhari RV, Subramaniam B. Catalytic hydroprocessing of P-cresol: metal, solvent and mass-transfer effects. *Topic Catal*. 2012;55(3):129-139.
3. Kim JS. Production, separation and applications of phenolic-rich bio-oil—a review. *Bioresour Technol*. 2015;178:90-98. https://doi.org/10.1016/j.biortech.2014.08.121.
4. Baloch HA, Nizamuddin S, Siddiqui M, et al. Recent advances in production and upgrading of bio-oil from biomass: a critical overview. *J Environ Chem Eng*. 2018;6(4):5101-5118. https://doi.org/10.1016/j.jece.2018.07.050.
5. Valle B, Remiro A, Garcia-Gomez N, Gayubo AG, Bilbao J. Recent research progress on bio-oil conversion into bio-fuels and raw chemicals: a review. *J Chem Technol Biotechnol*. 2019;94(3):670-689. https://doi.org/10.1002/jctb.5758.
6. Nie L, Resasco DE. Kinetics and mechanism of M-cresol hydrodeoxygenation on a Pt/SiO_2 catalyst. *J Catal*. 2014;317:22-29. https://doi.org/10.1016/j.jcat.2014.05.024.
7. Tan Q, Wang G, Nie L, et al. Different product distributions and mechanistic aspects of the hydrodeoxygenation of M-cresol over platinum and ruthenium catalysts. *ACS Catal*. 2015;5(11):6271-6283. https://doi.org/10.1021/acscatal.5b00765.
8. Wang C, Mironenko AV, Raizada A, et al. Mechanistic study of the direct hydrodeoxygenation of M-cresol over WO_x-decorated Pt/C catalysts. *ACS Catal*. 2018;8:7749-7759. https://doi.org/10.1021/acscatal.8b01746.
9. Li G, Han J, Wang H, Zhu X, Ge Q. Role of dissociation of phenol in its selective hydrogenation on Pt(111) and Pd(111). *ACS Catal*. 2015;5(3):2009-2016. https://doi.org/10.1021/cs501805y.
10. Gu GH, Mullen CA, Boateng AA, Vlachos DG. Mechanism of dehydration of phenols on Noble metals via first-principles microkinetic modeling. *ACS Catal*. 2016;6(5):3047-3055. https://doi.org/10.1021/acscatal.6b00776.
11. Teles CA, Rabelo-Neto RC, de Lima JR, Mattos LV, Resasco DE, Noronha FB. The effect of metal type on hydrodeoxygenation of phenol over silica supported catalysts. *Catal Lett*. 2016;146(10):1848-1857. https://doi.org/10.1007/s10562-016-1815-5.
12. Zhu X, Lobban LL, Mallinson RG, Resasco DE. Bifunctional transalkylation and hydrodeoxygenation of anisole over a Pt/HBeta catalyst. *J Catal*. 2011;281(1):21-29. https://doi.org/10.1016/j.jcat.2011.03.030.
13. Gao D, Xiao Y, Varma A. Guaiacol hydrodeoxygenation over platinum catalyst: reaction pathways and kinetics. *Ind Eng Chem Res*. 2015;54(43):10638-10644. https://doi.org/10.1021/acs.iecr.5b02940.
14. Han Y, Gholizadeh M, Tran CC, et al. Hydrotreatment of pyrolysis bio-oil: a review. *Fuel Process Technol*. 2019;195:106140. https://doi.org/10.1016/j.fuproc.2019.106140.
15. Bhanawase SL, Yadav GD. Activity and selectivity of Different Base catalysts in synthesis of guaifenesin from guaiacol and glycidol of biomass origin. *Catalysis Today*. 2017;291:213-222. https://doi.org/10.1016/j.cattod.2016.12.008.
16. Leiva K, Sepulveda C, Garcia R, et al. Kinetic study of the conversion of 2-methoxyphenol over supported re catalysts: sulfide and oxide state. *Appl Catal Gen*. 2015;505:302-308. https://doi.org/10.1016/j.apcata.2015.08.010.
17. Nimmanwudipong T, Runnebaum RC, Block DE, Gates BC. Catalytic conversion of guaiacol catalyzed by platinum supported on alumina: reaction network including hydrodeoxygenation reactions. *Energy Fuel*. 2011;25(8):3417-3427. https://doi.org/10.1021/ef200803d.
18. Runnebaum RC, Nimmanwudipong T, Block DE, Gates BC. Catalytic conversion of compounds representative of lignin-derived bio-oils: a reaction network for guaiacol, anisole, 4-methylanisole, and cyclohexanone

conversion catalysed by Pt/γ-Al_2O_3. *Cat Sci Technol*. 2012;2:113-118. https://doi.org/10.1039/C1CY00169H.

19. Bykova MV, Zavarukhin SG, Trusov LI, Yakovlev VA. Guaiacol hydrodeoxygenation kinetics with catalyst deactivation taken into consideration. *Kinet Catal*. 2013;54(1):40-48. https://doi.org/10.1134/S0023158413010023.
20. Wu SK, Lai PC, Lin YC, Wan HP, Lee HT, Chang YH. Atmospheric hydrodeoxygenation of guaiacol over alumina-, zirconia-, and silica-supported nickel phosphide catalysts. *ACS Sustain Chem Eng*. 2013;1(3):349-358. https://doi.org/10.1021/sc300157d.
21. Olcese RN, Francois J, Bettahar MM, Petitjean D, Dufour A. Hydrodeoxygenation of guaiacol, a surrogate of lignin pyrolysis vapors, over iron based catalysts: kinetics and modeling of the lignin to aromatics integrated process. *Energy Fuel*. 2013;27(2):975-984. https://doi.org/10.1021/ef301971a.
22. Fogler HS. *Elements of Chemical Reaction Engineering*. 4th ed. London, UK: Prentice Hall International, Inc; 2005.
23. Xiao Y, Varma A. Kinetics of glycerol conversion to hydrocarbon fuels over Pd/H-ZSM-5 catalyst. *AIChE J*. 2017;63(12):5445-5451. https://doi.org/10.1002/aic.15931.
24. Weekman VW Jr. Laboratory reactors and their limitations. *AIChE J*. 1974;20(5):833-840. https://doi.org/10.1002/aic.690200502.
25. Doraiswamy LK, Tajbl DG. Laboratory catalytic reactors. *Catal Rev*. 1974;10(1):177-219.
26. Christoffel EG. Laboratory reactors and heterogeneous catalytic processes. *Catal Rev*. 1982;24(2):159-232.
27. DiLeo GJ, Neff ME, Savage PE. Gasification of guaiacol and phenol in supercritical water. *Energy Fuel*. 2007;21(4):2340-2345. https://doi.org/10.1021/ef070056f.
28. Zhao H, Li D, Bui P, Oyama S. Hydrodeoxygenation of guaiacol as model compound for pyrolysis oil on transition metal phosphide hydroprocessing catalysts. *Appl Catal Gen*. 2011;391(1–2):305-310.
29. Gao D, Schweitzer C, Hwang HT, Varma A. Conversion of guaiacol on noble metal catalysts: reaction performance and deactivation studies. *Ind Eng Chem Res*. 2014;53(49):18658-18667.
30. Xiao Y, Greeley J, Varma A, Zhao ZJ, Xiao G. An experimental and theoretical study of glycerol oxidation to 1,3-dihydroxyacetone over bimetallic Pt-bi catalysts. *AIChE J*. 2017;63(2):705-715. https://doi.org/10.1002/aic.15418.
31. Xiao Y, Varma A. Bio-oil upgrading using methane: a mechanistic study of model compound guaiacol reactions over Pt-bi bimetallic catalysts. *ACS Sustain Chem Eng*. 2018;6(12):17368-17375. https://doi.org/10.1021/acssuschemeng.8b04925.
32. Chang J, Danuthai T, Dewiyanti S, Wang C, Borgna A. Hydrodeoxygenation of guaiacol over carbon-supported metal catalysts. *ChemCatChem*. 2013;5(10):3041-3049. https://doi.org/10.1002/cctc.201300096.
33. He P, Shan W, Xiao Y, Song H. Performance of Zn/ZSM-5 for in situ catalytic upgrading of pyrolysis bio-oil by methane. *Topic Catal*. 2016;59(1):86-93. https://doi.org/10.1007/s11244-015-0508-4.
34. Xiao Y, Varma A. Catalytic deoxygenation of guaiacol using methane. *ACS Sustain Chem Eng*. 2015;3(11):2606-2610. https://doi.org/10.1021/acssuschemeng.5b00669.
35. Perego C, Peratello S. Experimental methods in catalytic kinetics. *Catal Today*. 1999;52:133-145.
36. Weisz P, Prater C. Interpretation of measurements in experimental catalysis. *Adv Catal*. 1954;6:143-196.
37. Mears DE. Diagnostic criteria for heat transport limitations in fixed bed reactors. *J Catal*. 1971;20(2):127-131. https://doi.org/10.1016/0021-9517(71)90073-X.
38. Xiao Y, Varma A. Kinetics of guaiacol deoxygenation using methane over the Pt-bi catalyst. *React Chem Eng*. 2017;2(1):36-43. https://doi.org/10.1039/C6RE00187D.
39. Laurent E, Delmon B. Study of the hydrodeoxygenation of carbonyl, carboxylic and guaiacyl groups over sulfided CoMo/γ-Al_2O_3 and NiMo/γ-Al_2O_3 catalyst: I. catalytic reaction schemes. *Appl Catal Gen*. 1994;109(1):97-115. https://doi.org/10.1016/0926-860X(94)85005-4.
40. Lu J, Behtash S, Mamun O, Heyden A. Theoretical investigation of the reaction mechanism of the guaiacol hydrogenation over a Pt(111) catalyst. *ACS Catal*. 2015;5(4):2423-2435. https://doi.org/10.1021/cs5016244.
41. Bui VN, Laurenti D, Afanasiev P, Geantet C. Hydrodeoxygenation of guaiacol with CoMo catalysts. Part I: promoting effect of cobalt on HDO selectivity and activity. *Appl Catal Environ*. 2011;101(3–4):239-245.
42. Chiu CC, Genest A, Borgna A, Rosch N. Hydrodeoxygenation of guaiacol over Ru(0001): a DFT study. *ACS Catal*. 2014;4(11):4178-4188. https://doi.org/10.1021/cs500911j.
43. Bui VN, Laurenti D, Afanasiev P, Geantet C. Hydrodeoxygenation of guaiacol with CoMo catalysts. Part II: support effect for CoMoS catalysts on HDO activity and selectivity. *Appl Catal Environ*. 2011;101(3–4):246-255.
44. Lee K, Gu GH, Mullen CA, Boateng AA, Vlachos DG. Guaiacol hydrodeoxygenation mechanism on Pt(111): insights from density functional theory and linear free energy relations. *ChemSusChem*. 2015;8(2):315-322. https://doi.org/10.1002/cssc.201402940.
45. Nguyen TS, Laurenti D, Afanasiev P, Konuspayeva Z, Piccolo L. Titania-supported gold-based nanoparticles efficiently catalyze the hydrodeoxygenation of guaiacol. *J Catal*. 2016;344:136-140. https://doi.org/10.1016/j.jcat.2016.09.016.
46. Moon JS, Kim EG, Lee YK. Active sites of Ni_2P/SiO_2 catalyst for hydrodeoxygenation of Guaiacol: a joint XAFS and DFT study. *J Catal*. 2014;311:144-152. https://doi.org/10.1016/j.jcat.2013.11.023.

How to cite this article: Xiao Y, Lagare R, Blanshan L, Martinez EN, Varma A. Refinement of the kinetic model for guaiacol hydrodeoxygenation over platinum catalysts. *AIChE J*. 2020;e16913. https://doi.org/10.1002/aic.16913